ORIGINAL ARTICLE

Effect of Nitrogen-doped – Palm Oil Mill Effluent Sludge-biochar as Peroxydisulfate Activator on the Removal of Methylene Blue Dye as an Environmental-friendly Approach

Aida Humaira Sallehuddin[1], *Sabrina Karim[2], Mohamad Ali Ahmad[3], Tong Woei Yenn[4], and Noor Aina Mohd Nazri[5]

[1] Section of Environmental Healthcare, UniKL MESTECH, 43000 Kajang, Selangor, Malaysia
[2] Environmental Healthcare Research Cluster, Section of Environmental Healthcare, UniKL MESTECH, 43000 Kajang, Selangor, Malaysia
[3] School of Mechanical Engineering, College of Engineering, UiTM Shah Alam, 40450 Shah Alam, Selangor, Malaysia
[4] Clinical & Biomedical Laboratory Science Section, UniKL MESTECH, 43000 Kajang, Selangor, Malaysia
[5] Section of Chemical Engineering, UniKL MICET, 78000 Alor Gajah, Melaka, Malaysia

ABSTRACT

Introduction: Water pollution caused by dyes is a major problem as it is a toxic chemical that can cause chronic diseases when exposed to humans and aquatic habitats. Sulfate-based advanced oxidation process based on peroxydisulfate (PDS) has received a lot of attention recently for achieving color degradation in wastewater. Transition metal-based homogeneous/heterogeneous catalysts have shown to be a good alternative for the activation of persulfate. Nonetheless, this leads to significant secondary contamination due to metal leaching. Alternatively, nitrogen-doped biochar is a promising non-metal persulfate activator due to its lower cost and more environmentally friendly. **Methods:** Biochar from Palm Oil Mill Effluent (POME) sludge doped with nitrogen source of urea, ammonium chloride, and melamine was synthesized at a 700°C pyrolysis process and used to activate PDS. The nitrogen content of synthesized POME biochar was altered to ratios of 25:75, 50:50, and 75:25 respectively. Batch degradation experiments were then conducted to determine the feasibility of catalytic removal of methylene blue (MB) dye. **Results:** Based on experimental results, urea-doped biochar showed a greater MB removal compared to ammonium chloride and melamine-doped biochar. Besides that, higher nitrogen-to-biochar ratio increases the MB degradation significantly. A similar trend was demonstrated when a higher urea-doped biochar dosage was utilized. By utilizing 5.0 g of urea-doped biochar, a 100 ± 0.7% degradation of MB was achieved. **Conclusion:** This research provides an effective method to produce carbon-based catalysts from sludge recovery for activation of PDS, also enhancing the catalytic performance of biochar on MB dye removal by N-doping.
Malaysian Journal of Medicine and Health Sciences (2023) 19(SUPP9): 133-139. doi:10.47836/mjmhs.19.s9.20

Keywords: Wastewater; Palm oil mill effluent's sludge; Radical processes; Methylene blue; Advanced oxidation processes

Corresponding Author:
Sabrina Karim, PhD
Email: sabrinakarim@unikl.edu.my
Tel: +6019-3899244

INTRODUCTION

Due to rapid urbanization, a high number of toxic wastes are frequently discharged into the water. Synthetic dyes are one of the toxic wastes that can be found in wastewater. These dyes are widely utilized in many industries such as rubber, textiles, cosmetics, printing, and plastics. Water pollution caused by dyes is a great concern because it affects human and aquatic habitats even at a low concentration (1, 2). The presence of MB in water causes an increase in oxygen demand which then affects aquatic animals (2). It is estimated that over 700,000 tonnes of dyes are produced each year, mostly from the textile industries and about 2% of the dyes produced are discharged into the water systems (3). In the textile manufacturing process, methylene blue (MB) dye is widely used as a pH indicator and drug enhancer. However, only 5% of the MB dye is used and the remaining 95% is discharged as effluent (4). In recent years, various wastewater treatment technologies have emerged such as membrane separation (5), carbon adsorption (6), and advanced oxidation processes (AOP) (7) areused in wastewater treatment.

Among these methods, AOP is the most promising method for wastewater treatment as it works under extreme operating conditions, has lower costs, and are able to completely mineralize pollutants in the water (7). Strong oxidants such as hydroxyl radicals ($OH^{\cdot}$), sulfate radicals ($SO_4^{\cdot-}$), superoxide anion radicals ($O_2^{\cdot-}$), and singlet oxygen ($^1O_2$) are produced during AOP that destroy stubborn organic contaminants (8). This research focused on the AOP activation of sulfate radicals from peroxydisulfate (PDS). Due to their unique advantages, AOP based on sulfate radicals (SR-AOP) has progressively emerged (9). Sulfate radicals are thought to be more effective than hydroxyl radicals. Besides that, sulfate radicals have a higher half-life, higher oxidation potential, stronger selectivity, and are less affected by pH value compared to hydroxyl radicals (9). PDS is efficient oxidants, however, they are not able to decompose most stubborn organic substrates due to their low oxidation potential. Therefore, activation is required to produce free-radical or non-radical reactive species with higher reactivity than the persulfate parent in the persulfate/nanocarbon system (10). Numerous activation techniques of radical species have been reported in previous studies (10-13). Radiation such as ultraviolet (UV), ultrasound (US), and gamma rays (14) have been shown to be effective in activating persulfate, although the latter is not widely used.

Transition metal ions and metal oxides have been shown to be effective activators in activating PDS in degrading toxic and stubborn pollutants (12). In addition, organic and inorganic metal-containing linkers have also become an important precursor for preparing porous carbon materials for activating PDS (15). However, the use of this metal leads to the leaching of metal ions, limiting its applications (16). Therefore, a series of metal-free catalysts such as graphene oxide (GO), carbon nanotubes (CNT), and reduced graphene oxide (rGO) were developed to activate PDS (11, 17). These metal-free catalysts effectively avoid the problem of metal leaching; however, these metal-free catalysts lack sufficient active sites to break the O–O bond of PDS for radical generation, making the removal efficiency of organic contaminants not ideal (18). Therefore, carbon-based catalytic activation as a metal-free alternative yield excellent result (2, 3, 19). The main advantage of carbon-based materials is that they leave no residue in wastewater and can be reused many times before recovery is required (20). Biochar has emerged as a promising candidate to be used as a carbonaceous catalyst because it is environmentally friendly and sustainable (21). Nevertheless, the carbonaceous catalyst has limited application. To overcome this limitation, past studies have shown that doping heteroatoms such as sulfur (S), boron (B), nitrogen (N), and phosphorus (P) can enhance the catalytic activity of metal-free catalysts and decompose persistent organic pollutants (22). Comparing these heteroatoms, N-doped carbon materials have a large number of functional N groups and more vacancies, therefore exhibiting superior catalytic activity (23).

Currently, Malaysia is the world's leading palm oil exporter and producer. This has caused significant problems as palm oil mills produce large amounts of palm oil mill effluent (POME) (24). However, few studies have shown that POME sludge can be converted to biochar in high yields by low-temperature pyrolysis (25). Furthermore, another study also has proven that POME sludge can be utilised to produce solid char and liquid bio-oil using microwave-assisted pyrolysis (26). Therefore, N-doped POME sludge biochar has the potential to be used as a catalyst for the sulfate radical activator. This research aims to create an environmentally friendly activator that activates the sulfate radicals of PDS using natural resources. The aim of this study is also to produce low-cost nitrogen-doped biochar to catalyze the activation of PDS and determine the optimal conditions for the removal of MB.

MATERIALS AND METHODS

Biochar Preparation

POME sludge samples were collected from Felda Jengka, Pahang, and were then kept in an airtight container. The POME sample was dried in the sunlight for a day before being cleaned with distilled water three times. The samples were then dried for 24 hours at a drying oven temperature of 105 °C (27). Pyrolysis was carried out in a furnace for 4 hours at 700°C at a rate of heating of 10°C/min and the biochar was ground and sieved to get a smaller size. The biochar was then placed in the desiccators and kept in an air-tight container.

N-Doped Preparation

The biochar was nitrogen-doped using three different sources: ammonium chloride, urea, and melamine. Three ratios of N-doped biochar were prepared: 25:75, 50:50, and 75:25 respectively. 50 mL of ultrapure water was then poured into the mixture and was then placed into a 100 mL beaker. The solution was stirred for 8 hours. Then, the N-doped biochar was rinsed with distilled water three times and then oven-dried overnight at 60°C (28). The N-doped biochar was then heated to 350°C for 1 hour. The N-doped material was then taken from the furnace and allowed to cool until it reaches room temperature in the desiccator. Finally, the cooled N-doped sample was rinsed multiple times with distilled water and dried overnight at 60°C (21). After that, the dry N-doped material was stored in sealed glass bottles. This procedure was repeated for the remaining ratios of 50:50 and 75:25.

Characterization of Sample

Fourier transform infrared spectroscopy (FTIR) analysis was conducted to determine the functional groups and chemical characteristics of the biochar. The sample was firstly ground into powder and dried overnight i n the drying oven to remove any remaining moisture. The sample was then mixed with a potassium bromide (KBr) pellet (Sigma Aldrich) in a ratio of 1:100 and left to dry in a drying oven for 3 hours. The sample was then pressed into a hydraulic presser to form a pellet form (19). It was then analyzed using an FTIR analyzer with a wavelength of 400 cm^{-1} to 4000 cm^{-1}.

Batch Degradation Experiment

A 1000 mg/L MB stock solution was prepared in a 1-liter volumetric flask and altered to 3 different values: pH 3, pH 5, and pH 9. 250 mL conical flasks were prepared with MB solution alone (blank), MB and 100% biochar alone, MB and PDS alone, and MB, N-doped biochar and PDS alone. The conical flasks were closed and agitated for 180 minutes using an orbital shaker. The samples were withdrawn and filtered using a 0.45 µm syringe membrane filter. The reaction was then inhibited with the addition of 20 µL of methanol (29). The sample's absorbance was determined using a UV-Vis Spectrophotometer (Perkin Elmer) adjusted to 650 nm. This experiment was replicated to obtain an accurate and precise value. The experiments were repeated with varying N-doped biochar dosages.

RESULTS

Chemical Functional Group of Biochar by using FTIR analysis

The infrared spectra of absorption of the N-doped biochar samples were obtained using FTIR. FTIR was utilized to determine the functional group and chemical bonds of the POME biochar and N-doped biochar. A significant difference in peaks was observed before and after the N-doped process as illustrated in Fig. 1. Both POME biochar and N-doped POME biochar showed a peak at a wavelength of 3435 to 3450 cm^{-1}. Besides that, peaks at band 3000 to 3500 cm^{-1} which are the secondary amines group were also observed in all samples. Referring to Fig. 1, the N-doped POME biochar also exhibit peaks indicative of nitro compounds between wavelengths of 1383 to 1460 cm^{-1}. Besides that, wavelength peaks in the range of 1600 to 1700 cm^{-1} were also observed in the spectra of both raw POME biochar and nitrogen-doped biochar.

Effect of different nitrogen source doped biochar on the Degradation of MB by PDS

Fig. 2 illustrates the degradation of MB by using three different sources of N-doped biochar: urea-doped, ammonium chloride-doped, and melamine-doped. Based on the three nitrogen sources used, urea-doped

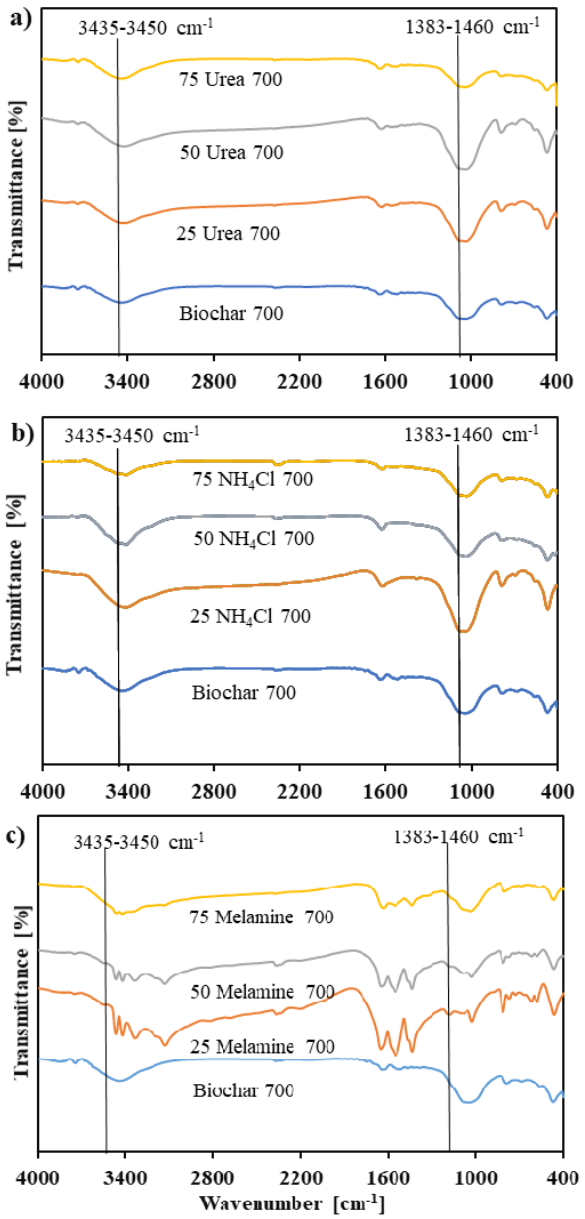

Fig. 1: The Fourier transform infrared spectroscopy (FTIR) spectrum for (a) urea-doped biochar, (b) ammonium chloride-doped biochar, (c) melamine-doped biochar ratio 25:75, 50:50, 75:25, and 100:0 (Biochar: Nitrogen source).

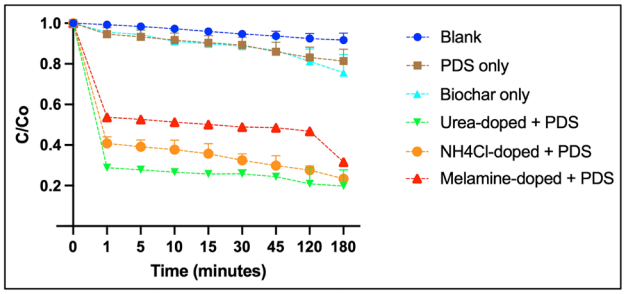

Fig. 2: Removal of methylene blue (MB) with different nitrogen sources [Experiment operating condition: MB initial concentration = 25 µM; Biochar dosage = 0.1 g; Initial pH = 3; PDS concentration = 6 mM; Pyrolysis temperature = 700 °C; Nitrogen: biochar ratio = 75:25].

biochar showed the most significant MB removal compared to ammonium chloride-doped biochar and melamine-doped biochar. Compared to these three nitrogen sources, by utilizing a 75% ratio of urea-doped biochar, the removal of MB achieved the highest MB removal with a percentage of 80.2 ± 2% after 180 minutes of reaction. Meanwhile, the removal of MB achieved by utilizing ammonium-chloride-doped biochar and melamine-doped biochar after 180 minutes were 76.7 ± 1.9% and 68.4 ± 0.8% respectively. This may relate to the FTIR spectra, where the most significant peaks of nitro compounds were observed in urea-doped biochar compared to ammonium chloride-doped biochar and melamine-doped biochar. Therefore, urea-doped biochar was utilized for further degradation experiments.

Effect of different nitrogen-doped ratios on the Degradation of MB by PDS

Fig. 3 illustrates the influence of nitrogen-doped biochar ratio on MB degradation. The nitrogen: biochar ratio employed in the experiment varies from 25 to 75%. Based on the figure, the degradation of MB by utilizing 100% biochar only achieved a degradation of 24.4 ± 2%. The urea-doped biochar ratio at 75% results in the highest MB degradation of 76.6 ± 0.6% after 180 minutes of reaction. Meanwhile, the degradation of MB achieved by utilizing 25 and 50% urea-doped biochar were 71.3 ± 1.8% and 74.1 ± 0.8% respectively.

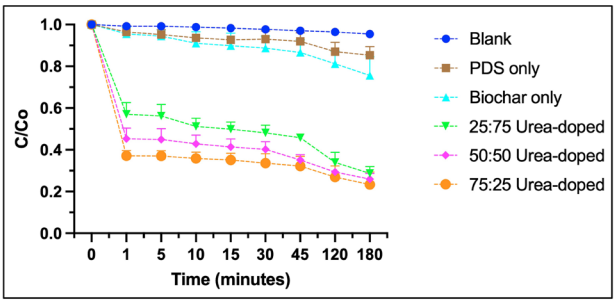

Fig. 3 : Removal of methylene blue (MB) with different urea-doped biochar ratio [Experiment operating condition: MB initial concentration = 25 µM; initial pH = 3; PDS concentration = 6 mM; Pyrolysis temperature = 700 °C; Biochar dosage = 0.1g].

Effect of Initial pH on the Degradation of MB by PDS

Fig. 4 illustrates the degradation of MB by using PDS with the addition of 75% urea-doped biochar at three different pH of 3, 5, and 9. After 180 minutes of reaction, the MB degradation at pH 3 achieved up to 80.2 ± 2%, whereas at pH 5 and pH 9, the MB degradation decreases and achieved the removal of 68.5 ± 1.7% and 67.6 ± 0.9% respectively. Based on the results, the optimum pH for MB degradation is pH 3.

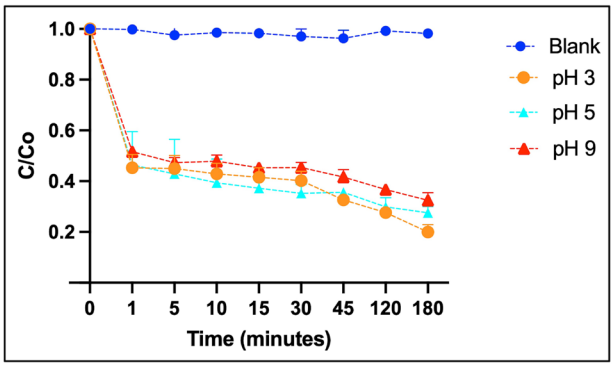

Fig. 4 : Removal of methylene blue (MB) at different initial pH [Experiment operating condition: MB initial concentration = 25 µM; Biochar dosage = 0.1 g; PDS concentration = 6 mM; Pyrolysis temperature = 700 °C; Urea: biochar ratio = 75:25].

Effect of different N-doped biochar dosages on the Degradation of MB by PDS

Fig. 5 illustrates the rate of MB degradation using various dosages of 100% biochar and 75% urea-doped biochar. Referring to the figure, it shows that increasing the biochar dosage from 0.1 g to 5.0 g improves the efficiency of MB degradation significantly. The urea-doped biochar dosage at 5.0 g results in the highest MB degradation of 100 ± 0.7%, whereas 0.1 g and 1.0 g of urea-doped biochar achieved a degradation of 80.1 ± 2% and 98.4 ± 0.8% respectively after 180 minutes of reaction.

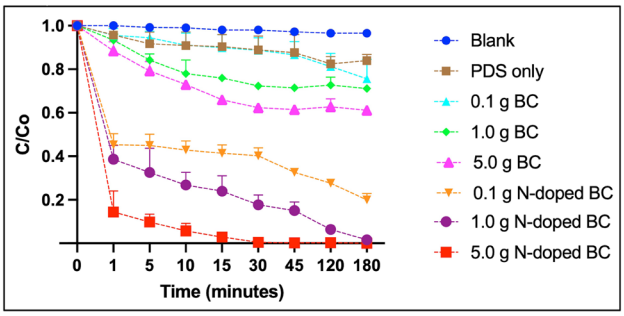

Fig. 5 : Removal of methylene blue (MB) at different biochar dosages [Experiment operating condition: MB initial concentration = 25 µM; initial pH = 3; PDS concentration = 6 mM; Pyrolysis temperature = 700 °C; Urea: biochar ratio = 75:25].

DISCUSSION

The FTIR spectra demonstrated that both POME biochar and N-doped POME biochar showed a significant quantity of oxygen-containing functional groups, such as the O-H stretching at a wavelength of 3435 to 3450 cm-1 (30). This may be related to the moisture content of the biochar and hydroxyl functional group of hemicellulose, cellulose, and lignin (31). Peaks at band 3000 to 3500 cm-1 which are the

secondary amines group were also observed in all samples (32). Referring to Fig. 1, the N-doped POME biochar exhibit peaks indicative of nitro compounds between wavelengths of 1383 to 1460 cm-1, suggesting that amides characteristic is present on the surface of the biochar (32). This stipulates successful nitrogen doping on the surface of the biochar. In addition, wavelength peaks in the range of 1600 to 1700 cm-1 were also observed in the spectra of both raw POME biochar and nitrogen-doped biochar. Peaks within this band correlate with the carboxylic acid groups of the biochar (21). However, the intensity of nitrogen-doped biochar is lower compared to raw biochar. This is because POME biochar has higher acidic functional group, whereas subjecting the nitrogen-doped biochar to the nitrogen-doped thermochemical process reduced the acidic functional groups of the nitrogen-doped biochar (21).

In this study, it was observed that by utilizing urea-doped biochar, helps to increase the efficiency of MB degradation. This is because as the urea content increased, the content of nitrogen surface-active sites in biochar also increased. The introduction and alteration of nitrogen species onto the biochar improves the adsorption capacity and increases the catalytic activation of PDS as it acted as the main active site (33). C-N bonds have a high anion-exchanging activity which promotes more positively charged atoms (10). These positively charged atoms are capable of generating active radical species thus improving catalytic capability (33).

The effect of initial pH on the degradation of MB by PDS was also studied. Based on the results, it is observed that as the pH increases, the adsorbent surfaces and contaminants become more positively charged. Thus, it reduces the electrostatic interaction between MB and the negative functional groups of the N-doped biochar, simultaneously decreasing the efficiency of MB degradation (27). In general, the catalytic reaction was more efficient under acidic conditions compared to alkaline conditions. Samal et al also proposed a similar outcome where the degradation of MB was the highest at pH ranging from 3 to 4 (34).

Different N-doped biochar dosages was also used to determine the effect on MB degradation. Based on the results, it shows that increasing the biochar dosage from 0.1 g to 5.0 g gives a significant increase on the removal efficiency of MB. This finding attribute to the fact that a large amount of biochar provides more active sites for the PDS activation, resulting in more generation of reactive oxygen species (ROS), simultaneously increasing MB degradation efficiency (35).

CONCLUSION

The biochar from POME sludge was prepared and was nitrogen-doped with three nitrogen sources: urea, ammonium chloride, and melamine with ratios of 25, 50, and 75%. The N-doped biochar was utilized as a catalyst in PDS activation to enhance MB degradation. Based on experimental results, the nitrogen doping was successful by utilizing the three nitrogen sources, with 1.0 g of urea-doped biochar producing the highest MB degradation at 80.2 ± 2% after 180 minutes of reaction. Besides that, 5.0 g of 75% urea-doped biochar achieved 100 ± 0.7% degradation of MB after 180 minutes of reaction. The increase in biochar dosage and biochar ratios also simultaneously increased the efficiency of MB degradation. It can be concluded that the addition of nitrogen species produced more active sites for PDS activation, simultaneously enhancing MB degradation. This work exhibits great potential in utilizing POME carbocatalyst incorporate with nitrogen precursor to enhance the activation of PDS to replaced metal-based catalyst. This green-carbocatalyst is a scalable and cost-effective method to develop a sustainable low-cost catalyst and simultaneously reducing secondary contamination in wastewater due to metal leaching of metal-based catalysts.

ACKNOWLEDGMENT

This research was supported financially by the Ministry of Higher Education, Malaysia under the grant of FGRS/1/2020/STG05/UNIKL/02/4.

REFERENCES

1. Ahmad MA, Eusoff MA, Oladoye PO, Adegoke KA, Bello OS. Optimization and batch studies on adsorption of Methylene blue dye using pomegranate fruit peel based adsorbent. Chemical Data Collections. 2021;32:100676. doi: 10.1016/j.cdc.2021.100676.
2. Mohamed F, Shaban M, Zaki SK, Abd-Elsamie MS, Sayed R, Zayed M, et al. Activated carbon derived from sugarcane and modified with natural zeolite for efficient adsorption of methylene blue dye: experimentally and theoretically approaches. Scientific Reports. 2022;12(1):1-18. doi: 10.1038/s41598-022-22421-8.
3. Auta M, Hameed B. Preparation of waste tea activated carbon using potassium acetate as an activating agent for adsorption of Acid Blue 25 dye. Chemical engineering journal. 2011;171(2):502-9. doi: 10.1016/j.cej.2011.04.017.
4. Lin D, Wu F, Hu Y, Zhang T, Liu C, Hu Q, et al. Adsorption of dye by waste black tea powder: parameters, kinetic, equilibrium, and

thermodynamic studies. Journal of Chemistry. 2020;2020. doi: 10.1155/2020/5431046.
5. Obotey Ezugbe E, Rathilal S. Membrane technologies in wastewater treatment: a review. Membranes. 2020;10(5):89. doi: 10.3390/membranes10050089.
6. Cao J, Yang Z-h, Xiong W-p, Zhou Y-y, Peng Y-r, Li X, et al. One-step synthesis of Co-doped UiO-66 nanoparticle with enhanced removal efficiency of tetracycline: Simultaneous adsorption and photocatalysis. Chemical Engineering Journal. 2018;353:126-37. doi: 10.1016/j.cej.2018.07.060.
7. Vallejo M, San Rom6n MF, Ortiz I, Irabien A. Overview of the PCDD/Fs degradation potential and formation risk in the application of advanced oxidation processes (AOPs) to wastewater treatment. Chemosphere. 2015;118:44-56. doi: 10.1016/j.chemosphere.2014.05.077.
8. Du J, Kim SH, Hassan MA, Irshad S, Bao J. Application of biochar in advanced oxidation processes: supportive, adsorptive, and catalytic role. Environmental Science and Pollution Research. 2020;27(30):37286-312. doi: 10.1007/s11356-020-07612-y.
9. Zhao C, Shao B, Yan M, Liu Z, Liang Q, He Q, et al. Activation of peroxymonosulfate by biochar-based catalysts and applications in the degradation of organic contaminants: A review. Chemical Engineering Journal. 2021;416:128829. doi: 10.1016/j.cej.2021.128829.
10. Chen X, Oh W-D, Lim T-T. Graphene-and CNTs-based carbocatalysts in persulfates activation: Material design and catalytic mechanisms. Chemical Engineering Journal. 2018;354:941-76. doi: 10.1016/j.cej.2018.08.049.
11. Ozyildiz G, Olmez-Hanci T, Arslan-Alaton I. Effect of nano-scale, reduced graphene oxide on the degradation of bisphenol A in real tertiary treated wastewater with the persulfate/UV-C process. Applied Catalysis B: Environmental. 2019;254:135-44. doi: 10.1016/j.apcatb.2019.04.092.
12. Pi Z, Li X, Wang D, Xu Q, Tao Z, Huang X, et al. Persulfate activation by oxidation biochar supported magnetite particles for tetracycline removal: Performance and degradation pathway. Journal of Cleaner Production. 2019;235:1103-15. doi: 10.1016/j.jclepro.2019.07.037.
13. Wang J, Wang S. Activation of persulfate (PS) and peroxymonosulfate (PMS) and application for the degradation of emerging contaminants. Chemical Engineering Journal. 2018;334:1502-17. doi: 10.1016/j.cej.2017.11.059.
14. Wang S, Wang J. Degradation of carbamazepine by radiation-induced activation of peroxymonosulfate. Chemical Engineering Journal. 2018;336:595-601. doi: 10.1016/j.cej.2017.12.068.
15. Chen X, Wang N, Shen K, Xie Y, Tan Y, Li Y. MOF-derived isolated Fe atoms implanted in N-doped 3D hierarchical carbon as an efficient ORR electrocatalyst in both alkaline and acidic media. ACS applied materials & interfaces. 2019;11(29):25976-85. doi: 10.1021/acsami.9b07436.
16. Pang YL, Abdullah AZ. Current status of textile industry wastewater management and research progress in Malaysia: a review. Clean–Soil, Air, Water. 2013;41(8):751-64. doi: 10.1002/clen.201000318.
17. Yao F, Yang Q, Zhong Y, Shu X, Chen F, Sun J, et al. Indirect electrochemical reduction of nitrate in water using zero-valent titanium anode: Factors, kinetics, and mechanism. Water research. 2019;157:191-200. doi: 10.1016/j.watres.2019.03.078.
18. Oh W-D, Lim T-T. Design and application of heterogeneous catalysts as peroxydisulfate activator for organics removal: an overview. Chemical Engineering Journal. 2019;358:110-33. doi: 10.1016/j.cej.2018.09.203.
19. Duan X, Ao Z, Li D, Sun H, Zhou L, Suvorova A, et al. Surface-tailored nanodiamonds as excellent metal-free catalysts for organic oxidation. Carbon. 2016;103:404-11. doi: 10.1016/j.carbon.2016.03.034.
20. Shariff A, Aziz NSM, Abdullah N. Slow pyrolysis of oil palm empty fruit bunches for biochar production and characterisation. Journal of Physical Science. 2014;25(2):97. doi.
21. Razali N, Kamarulzaman NZ. Chemical characterizations of biochar from palm oil trunk for palm oil mill effluent (POME) treatment. Materials Today: Proceedings. 2020;31:191-7. doi: 10.1016/j.matpr.2020.02.219.
22. Zhou X, Zeng Z, Zeng G, Lai C, Xiao R, Liu S, et al. Persulfate activation by swine bone char-derived hierarchical porous carbon: multiple mechanism system for organic pollutant degradation in aqueous media. Chemical Engineering Journal. 2020;383:123091. doi: 10.1016/j.cej.2019.123091.
23. Zhang X, Wang Y, Du Y, Qing M, Yu F, Tian ZQ, et al. Highly active N, S co-doped hierarchical porous carbon nanospheres from green and template-free method for super capacitors and oxygen reduction reaction. Electrochimica Acta. 2019;318:272-80. doi: 10.1016/j.electacta.2019.06.081.
24. Muda K, Ezechi EH. Overview of trends in crude palm oil production and economic impact in Malaysia. Sriwijaya Journal of Environment. 2019;4(1):19-26. doi: 10.22135/sje.2019.4.1.19.
25. Thangalazhy-Gopakumar S, Al-Nadheri WMA, Jegarajan D, Sahu J, Mubarak N, Nizamuddin S. Utilization of palm oil sludge through pyrolysis for bio-oil and bio-char production. Bioresource technology. 2015;178:65-9. doi: 10.1016/j.biortech.2014.09.068.
26. Januri Z, Rahman N, Idris S, Matali S, Manaf S, Faris N, et al. Effect of activated carbon as microwave

absorbance on the yields of microwave assisted pyrolysis of palm oil mill effluent. 2014. doi: 10.1049/cp.2014.1456.
27. Mashkoor F, Nasar A. Magsorbents: Potential candidates in wastewater treatment technology–A review on the removal of methylene blue dye. Journal of magnetism and magnetic materials. 2020;500:166408. doi: 10.1016/j.jmmm.2020.166408.
28. Jindo K, Mizumoto H, Sawada Y, Sanchez-Monedero MA, Sonoki T. Physical and chemical characterization of biochars derived from different agricultural residues. Biogeosciences. 2014;11(23):6613-21. doi: 10.5194/bg-11-6613-2014.
29. Yin H, Yao F, Pi Z, Zhong Y, He L, Hou K, et al. Efficient degradation of bisphenol A via peroxydisulfate activation using in-situ N-doped carbon nanoparticles: Structure-function relationship and reaction mechanism. Journal of Colloid and Interface Science. 2021;586:551-62. doi: 10.1016/j.jcis.2020.10.120.
30. Chia CH, Gong B, Joseph SD, Marjo CE, Munroe P, Rich AM. Imaging of mineral-enriched biochar by FTIR, Raman and SEM–EDX. Vibrational Spectroscopy. 2012;62:248-57. doi: 10.1016/j.vibspec.2012.06.006.
31. Lamaming J, Hashim R, Sulaiman O, Leh CP, Sugimoto T, Nordin NA. Cellulose nanocrystals isolated from oil palm trunk. Carbohydrate Polymers. 2015;127:202-8. doi: 10.1016/j.carbpol.2015.03.043.
32. Zhou Q, Jiang X, Li X, Jia CQ, Jiang W. Preparation of high-yield N-doped biochar from nitrogen-containing phosphate and its effective adsorption for toluene. RSC advances. 2018;8(53):30171-9. doi: 10.1039/C8RA05714A
33. Zaeni JRJ, Lim J-W, Wang Z, Ding D, Chua Y-S, Ng S-L, et al. In situ nitrogen functionalization of biochar via one-pot synthesis for catalytic peroxymonosulfate activation: Characteristics and performance studies. Separation and Purification Technology. 2020;241:116702. doi: 10.1016/j.seppur.2020.116702.
34. Samal DP. Characterization of activated carbon and study of adsorption of methylene blue dye using activated carbon 2014.
35. Li W, Liu B, Wang Z, Wang K, Lan Y, Zhou L. Efficient activation of peroxydisulfate (PDS) by rice straw biochar modified by copper oxide (RSBC-CuO) for the degradation of phenacetin (PNT). Chemical Engineering Journal. 2020;395:125094. doi: 10.1016/j.cej.2020.125094.